SAE 2021-01-1158

Performance Comparison of LPG and Gasoline in an Engine Configured for EGR-Loop Catalytic Reforming

Author, co-author (Do NOT enter this information. It will be pulled from participant tab in MyTechZone)

Affiliation (Do NOT enter this information. It will be pulled from participant tab in MyTechZone)

Abstract

In prior work, the EGR loop catalytic reforming strategy developed by ORNL has been shown to provide a relative brake engine efficiency increase of more than 6% by minimizing the thermodynamic expense of the reforming processes, and in some cases achieving thermochemical recuperation (TCR), a form of waste heat recovery where waste heat is converted to usable chemical energy. In doing so, the EGR dilution limit was extended beyond 35% under stoichiometric conditions. In this investigation, a Microlith®-based metal-supported reforming catalyst (developed by Precision Combustion, Inc. (PCI)) was used to reform the parent fuel in a thermodynamically efficient manner into products rich in H_2 and CO. We were able to expand the speed and load ranges relative to previous investigations: from 1,500 to 2,500 rpm, and from 2 to 14 bar break mean effective pressure (BMEP). Experiments were conducted to determine the effects of the H/C ratio of the fuel on H_2 production and on the engine efficiency in order to compare E10 gasoline (H/C = 1.95) and liquified petroleum gas (LPG), comprised primarily of propane (H/C = 2.67). Additionally, the compression ratio of the engine was increased to ascertain whether further efficiency improvements could be realized based on a reduced knock propensity of the dilute EGR mixture with the reformed fuel. Both the gasoline and propane reforming strategies provided efficiency gains up to 1.85 percentage points and further efficiency improvements with the increased compression ratio were realized. The fuel specific effects of gasoline vs. LPG, the effect of engine operating condition on reforming, and knock limits of the reformed mixture are discussed in detail.

Introduction

This manuscript is a continuation of previous exhaust gas recirculation (EGR) loop reforming investigations from Oak Ridge National Laboratory (ORNL). As a result, much of the background information has been described previously [1-4], but is updated and included here for completeness.

Efficiency improvements in spark-ignited engines are desired as a pathway to meet increasingly challenging fuel economy and CO_2 emission regulations [5]. External cooled EGR provides known thermodynamic benefits while maintaining compatibility with conventional three-way catalysts (TWCs) for emissions control [6]. Caton [7] summarized the thermodynamic benefits of EGR, which include reduced pumping work at part-load conditions, decreased heat transfer due to lower cylinder temperature, and increased ratio of specific heats. External EGR is also a proven way to decrease the knocking propensity for a given fuel, which can be used as the basis for additional increases in efficiency through more advanced combustion phasing or higher compression ratio [8], though the extent of the knock mitigation potential of EGR is operating condition dependent [9, 10]. EGR was also shown to reduce NOx emissions over a broad range of speed and load conditions [11, 12].

The amount of EGR dilution that can be used is limited due to cycle-to-cycle combustion instability, thereby limiting the potential efficiency benefit of EGR [13-15]. EGR dilution causes a reduction in flame speed and elongates the initial flame kernel development process, making it more susceptible to stochastic turbulence variation, resulting in high cyclic variability [9, 16, 17]. While there are numerous other technologies being developed to extend the EGR dilution limit, this work focuses primarily on extending the EGR dilution limit with fuel reforming.

The addition of the major products of fuel reforming, specifically H_2, increases the combustion rate and can increase engine efficiency because of the shorter combustion duration [18-24]. Alger et al. [25] reported that H_2 can also be used to extend the EGR dilution limit, with the addition of 1 vol % H_2 extending the EGR limit from 25% to more than 50% for gasoline and from 20% to 28% for compressed natural gas. Fennell et al. [26] showed that simulated H_2-rich

[1] **Disclaimer:** This manuscript has been authored by UT-Battelle, LLC, under Contract No. DE-AC0500OR22725 with the US Department of Energy (DOE). The US government retains and the publisher, by accepting the article for publication, acknowledges that the US government retains a nonexclusive, paid-up, irrevocable, worldwide license to publish or reproduce the published form of this manuscript, or allow others to do so, for US government purposes. DOE will provide public access to these results of federally sponsored research in accordance with the DOE Public Access Plan (http://energy.gov/downloads/ doe-public-access-plan).

reformate could extend EGR dilution in an SI engine from 21% to 27% at the same combustion stability.

Though there are many approaches to generate reformate onboard, they can generally be classified into two broad categories. The first category is where fuel is reformed in one or more cylinders in an engine using noncatalytic processes. This category includes the Dedicated EGR (D-EGR) strategy developed by Southwest Research Institute, which is the most developed strategy in this category [27-29]. The second category of fuel reforming, and the category of the present work, is where a catalyst is used to reform the fuel outside of the engine cylinders [23, 26, 30-39].

Catalytic reforming processes often use the sensible enthalpy in the exhaust to promote reforming reactions over the catalyst to improve the energetics of reforming [22, 23, 30-33, 38-40]. The range of possible combustion and reforming reactions that can occur has been previously presented by Ahmed and Krumpelt [41] and by Jamal and Wyszynski [22] and are summarized here using iso-octane as the starting fuel. Equation 1 below shows the reaction stoichiometry for the complete combustion of iso-octane, while Equation 2 defines equivalence ratio (Φ). For the purposes of this manuscript, Φ refers to the O_2/Fuel ratio of complete combustion in Equation 1 relative to the actual O_2/Fuel ratio. This definition of Φ is equivalent to the more standard definition based on air instead of O_2, but an air-based Φ could not be used since fuel-lean engine exhaust rather than air is entering the catalyst. Equations 3–5 show the primary types of reactions that can occur in a reformer. When O_2 is present in quantities less than that required for complete combustion, partial oxidation (POx) occurs where the parent hydrocarbon is converted to syngas (CO and H_2), resulting in an exothermic process as shown in equation 3. For an environment devoid of O_2 but where H_2O is present, the resultant steam reforming reaction, shown in equation 4, is highly endothermic and results in much higher concentrations of H_2. Similarly, equation 5 shows a dry reforming reaction where CO_2 is consumed to form H_2 and CO in a process that is substantially more endothermic than steam reforming, but where the concentrations of H_2 are lower. Ideally, the endothermic reforming reactions in Equations 4 and 5 are driven by the sensible enthalpy in the exhaust, allowing for waste heat recovery through thermochemical recuperation (TCR) [42].

Complete Combustion: $C_8H_{18} + 12.5\ O_2 \rightarrow 8\ CO_2 + 9\ H_2O$ (- 5050.2 kJ/mol) (1)

Equivalence Ratio: $$\Phi = \frac{\left({}^{O_2}/_{Fuel}\right)_{Complete\ Combustion}}{\left({}^{O_2}/_{Fuel}\right)_{actual}} \quad (2)$$

POx Reforming: $C_8H_{18} + 4\ O_2 \rightarrow 8\ CO + 9\ H_2$ (−660.4 kJ/mol) (3)

Steam Reforming: $C_8H_{18} + 8\ H_2O \rightarrow 8\ CO + 17\ H_2$ (+1,274.2 kJ/mol) (4)

Dry Reforming: $C_8H_{18} + 8\ CO_2 \rightarrow 16\ CO + 9\ H_2$ (+1,603.8 kJ/mol) (5)

It is challenging to operate the engine and catalyst reforming system together to obtain robust operation and produce an increase in engine efficiency. Hwang et al.integrated a reforming catalyst containing Rh and Pt into the exhaust manifold of a diesel engine. While they were able to produce high concentrations of H_2 (> 10%), the reforming system resulted in an overall engine efficiency decrease because the reformer catalyst Φ was too low (as low as 1.5), and the reforming process was too dependent on the exothermic reactions in equation 3. This is consistent with much of the diesel reforming work where high concentrations of H_2 can be produced, but because of the dependency on POx reforming, there is a large fuel energy penalty to produce the H_2 [43, 44]. In contrast, Ashida et al. [30] used a steam reforming catalyst (4 wt% Rh/Al_2O_3, La additive) in the EGR loop of a spark ignition engine without any additional O_2 (catalyst Φ approaching ∞). They initially found high levels of fuel conversion and H_2 production, but the steam reforming catalyst began deactivating immediately, with a 35 ppm S fuel resulting in a 90% deactivation within 5 hours.

In our prior work [1-4], we focused on identifying reformer boundary conditions (primarily, O_2 and Φ at the catalyst inlet) such that the reforming process was both thermodynamically favorable and robust. Both flow reactor studies [3] and on-engine catalyst investigations [1] found that the most thermodynamically favorable reforming conditions occurred at low O_2 concentrations (~2 %) and high catalyst Φ (~7–9), but these were not necessarily the conditions that produced the highest reforming fuel conversion or H_2 concentrations. We confirmed that these thermodynamically favored reforming conditions also produced the highest engine efficiency benefits [2, 4], with the efficiency benefits being dependent on the speed and load operating condition. A relative efficiency improvement of more than 6% was achieved at some operating conditions.

In this study, we investigated three additional aspects of the EGR-loop reforming strategy:

1. Determine whether a fuel with a higher H/C ratio, in this case liquified petroleum gas (LPG, H/C = 2.67), provides reforming benefits relative to gasoline (H/C = 1.95), either thermodynamically or in terms of higher H_2 generation.
2. Pursue further speed-load range expansion and determine what barriers exist to full operating map implementation of this combustion strategy.
3. Exploit the improved knock mitigation of the dilute EGR reformate mixture by increasing the compression ratio (r_c) from the stock configuration of 9.2:1 to 11.85:1 to further increase engine efficiency.
4. Evaluate an advanced catalyst design that is tolerant of fuel contaminants and rapid thermal cycles and confirm that it does not show the degradation reported by others.

The present investigation limits the reforming boundary conditions to those that were previously identified as being thermodynamically advantageous: catalyst inlet O_2 concentration of 2.0 ± 0.2%, and catalyst Φ of 8.0 ± 1.0.

Experimental Methods

Fuels Investigated

Two fuels were used in this investigation. The first fuel was Euro EEE Stage VI Gasoline, Haltermann product code HF2017. It is a full boiling range premium-grade gasoline containing 10% ethanol with the specifications shown in Table 1. This fuel was chosen because it was desirable to have a full boiling range gasoline containing a realistic H/C, and with aromatic and olefinic content representative of commercial gasoline. It was also desirable to use fuel containing as little sulfur as possible, in this case 2 mg/kg.

The second fuel was commercially available LPG, which is also sold as Autogas for vehicle applications. The LPG was delivered to ORNL from a local supplier that makes residential and commercial deliveries of LPG. The composition of the LPG used in these experiments was not measured directly, but for reference, the average

fuel properties of LPG from a survey of 50 samples in the U.S. [45] are shown in Table 2.

Table 1. Fuel Properties of Euro EEE Stage VI Gasoline.

RON [-]	ASTM D2699	97.6
MON [-]	ASTM D2700	86.7
Anti-knock index (AKI) [-]	N/A	92.2
Ethanol [vol %]	ASTM D4815	9.5
Carbon [wt %]	ASTM D5291	83.03
Hydrogen [wt %]	ASTM D5291	13.49
Oxygen [wt %]	ASTM D4815	3.48
Net Heating Value [MJ/kg]	ASTM D240	41.5
Sulfur [mg/kg]	ASTM D5453	2
Aromatics [vol %]	ASTM D1319	28.4
Olefins [vol %]	ASTM D1319	8.2
Saturates [vol%]	ASTM D1319	53.9
Initial boiling point [°C]	ASTM D86	37
10% distillation [°C]	ASTM D86	54
50% distillation [°C]	ASTM D86	86
90% distillation [°C]	ASTM D86	155
Distillation end point [°C]	ASTM D86	174

Table 2. Average fuel properties of LPG in the U.S. [45].

RON [-]	Calculated[1]	109.1 ± 0.2
MON [-]	Calculated[1]	96.2 ± 0.1
Anti-knock index (AKI) [-]	N/A	102.7
Methane [vol %]	ASTM D2163	0.01 ± 0.02
Ethane [vol %]	ASTM D2163	2.48 ± 1.62
Propane [vol %]	ASTM D2163	96.06 ± 1.78
Iso-butane [vol %]	ASTM D2163	0.96 ± 0.77
n-butane [vol %]	ASTM D2163	0.18 ± 0.24
Net Heating Value [MJ/kg]	ASTM D240	46.4
Hydrogen [wt %]	Calculated	18.20
Carbon [wt %]	Calculated	81.80

Experimental Facility

This investigation is a continuation of prior engine experimental work using the EGR-loop catalytic reforming strategy [1, 2, 4], and as a result, many of the experimental methods are carried over from the prior investigations.

A 2.0 L GM Ecotec LNF SI engine equipped with the production side-mounted direct injection fueling system was used in this investigation. Engine geometry details are presented in Table 3. Two different r_c configurations were used. The first used the stock r_c = 9.2:1 configuration for the baseline SI performance and the initial EGR-loop studies. The second r_c configuration utilized a high r_c = 11.85:1 in three of the cylinders while maintaining the stock r_c = 9.2:1 in the fourth cylinder. The higher r_c piston was originally designed by Moore et al. [46]. The intake and exhaust camshaft profiles were unchanged from the stock configuration.

Engine experiments were performed using a motoring dynamometer and operating conditions are reported on a brake mean effective pressure (BMEP) basis. The engine torque was measured with a load cell on the engine dynamometer. In all cases, the engine exhaust was held to stoichiometric conditions to maintain compatibility with a conventional TWC for emissions control. Additionally, the combustion phasing midpoint (CA50) for all cylinders was held at 8 CA deg after firing top dead center ($aTDC_f$) by adjusting individual cylinder spark timing unless limited by end gas knock, in which case combustion was phased later in the cycle to avoid knock. Gross indicated mean effective pressure (IMEP) was balanced between the four cylinders by adjusting individual cylinder fuel injection duration.

Compressed and dried facility air having less than 5% relative humidity was used in this investigation. The air was delivered to the engine using a series of mass flow controllers from Alicat. The mass air flow controllers consisted of maximum ranges of 5000 slpm (MCRH-5000SLPM), 1,500 slpm (MCP-1500SLPM), and 500 slpm (MCP-500SLPM). As will be discussed, the reforming conditions had an isolated air supply path for cylinder 4, so reforming operating conditions utilize two mass flow controllers for each condition. The intake manifold temperature was controlled to a constant temperature of 35°C for all conditions using an electric heater.

While facility air enables boosted engine operation, it was desirable to apply backpressure on the engine exhaust to maintain reasonable air handling boundary conditions. This was done by using a 2" electromechanical ball valve from Flowserve with a characterized seat for proportional control. Under boosted operating conditions, the backpressure was adjusted to achieve a simulated turbocharger efficiency of 40% using the methodology describe by Trenc et al.[47]. Using a constant combined turbocharger efficiency is similar to the approach presented by Chadwell et al. [48] to compare air handling requirements for several different combustion strategies.

Engine control was performed using the National Instruments Powertrain Controls platform. This allowed control of cam phasing for the engine and of fuel and spark parameters on an individual-cylinder basis. Combustion analysis was done using software developed in-house, Oak Ridge Combustion Analysis System. For each experimental condition, cylinder pressure, spark discharge, and camshaft position data were recorded at 0.2 °CA resolution for 500 consecutive cycles. Cylinder pressure was measured using a flush-mounted piezoelectric pressure transducer from Kistler (6125C) in each cylinder, and camshaft position was obtained from the production Hall-effect sensors. DI fuel injection timing started during the intake stroke and was held constant at 280 °CA before firing top dead center ($bTDC_f$). The in-pipe catalyst fueling was delivered with the PFI start of injection at 170 °CA after firing top dead center ($aTDC_f$) in cylinder 4, so that fuel injection occurred shortly after exhaust valve opening.

Table 3. Engine Geometry

Bore × stroke [mm]	86.0 × 86.0
Conrod length [mm]	145.5
Wrist pin offset toward expansion stroke[mm]	0.8
Compression ratio [-]	9.2:1; 11.85:1
Fuel injection system	Direct injection, side-mounted, production injector with opposite linear wall–directed six-hole spray pattern

For the DI fueling with gasoline in both the conventional and reforming configurations, gasoline fuel was delivered to the engine at 5 bar pressure using an automotive PFI lift pump, and a Micromotion CMF010 Coriolis effect flow meter provided a total fuel flow measurement. The direct-injection fuel was delivered to the stock cam-driven fuel pump, which was used to maintain a constant rail

pressure of 125 bar for engine loads 4 bar BMEP and greater, but a lower pressure of 75 bar was required for the 2 bar BMEP operating condition so that the fuel injection duration could be sufficiently long for repeatable operation. For the reforming experiments with gasoline, a portion of the total fuel was sent through a second Micromotion CMF010 Coriolis flow meter and then to the water-cooled PFI injector located in the cylinder 4 exhaust. This provided a direct measurement of the catalyst in-pipe fueling.

LPG was delivered to the GDI fuel rail of the engine at the desired rail pressure, bypassing the stock cam-driven fuel pump. This was accomplished by supplying liquid propane from the LPG tank, which has a nominal pressure of 8-10 bar depending on the ambient temperature, and then cooling the liquid fuel to 0°C using a chiller and heat exchanger arrangement to prevent boiling during pumping. Immediately at the outlet of the heat exchanger, the LPG was supplied to an electrically-driven piston style positive displacement pump from CheckPoint Pumps & Systems (Model FA31-C1VD FXA 1500) to pump the fuel to the desired rail pressure. The pressurized LPG fuel was coupled to a bladder-style hydraulic accumulator before being sent through the Micromotion CMF010 Coriolis flow meter. The electric motor driving the positive displacement pump was controlled using a closed-loop PID controller to maintain a constant rail pressure of 100 bar at the GDI rail, with the exception of the 2 bar BMEP engine conditions, where a lower pressure of 75 bar was used to ensure fuel injector repeatability. Note that the reduced rail pressure of 100 bar used for the LPG relative to the 125 bar for the gasoline was due to the pressure rating of the Micromotion Coriolis flow meter.

This engine was operated in both the conventional SI configuration (no EGR) and with an EGR-loop catalytic reforming strategy. For the reforming strategy, the intake and exhaust manifolds were reconfigured to have cylinder 4 isolated from the remaining cylinders. The exhaust from this cylinder is mixed with fuel from an in-pipe catalyst fueling system to feed the reforming catalyst prior to passing through the EGR cooler and entering the intake plenum and static mixer arrangement, thereby providing the entirety of the reformate-EGR mixture to the other three cylinders. Cylinder 4 does not have the ability to breathe the EGR-reformate mixture as the other cylinders do. However, because the entirety of the cylinder 4 exhaust feeds the reforming catalyst and is recirculated to the other three cylinders, it is not necessary to maintain stoichiometric conditions in cylinder 4 to have a stoichiometric exhaust. As discussed in the introduction section, the catalyst inlet conditions were held at an inlet O_2 concentration of 2.0 ± 0.2%, and catalyst Φ of 8.0 ± 1.0 based on findings from our prior work [1-4]. The overall schematic of the engine flows, showing the isolated intake and exhaust for cylinder 4, is shown in Figure 1.

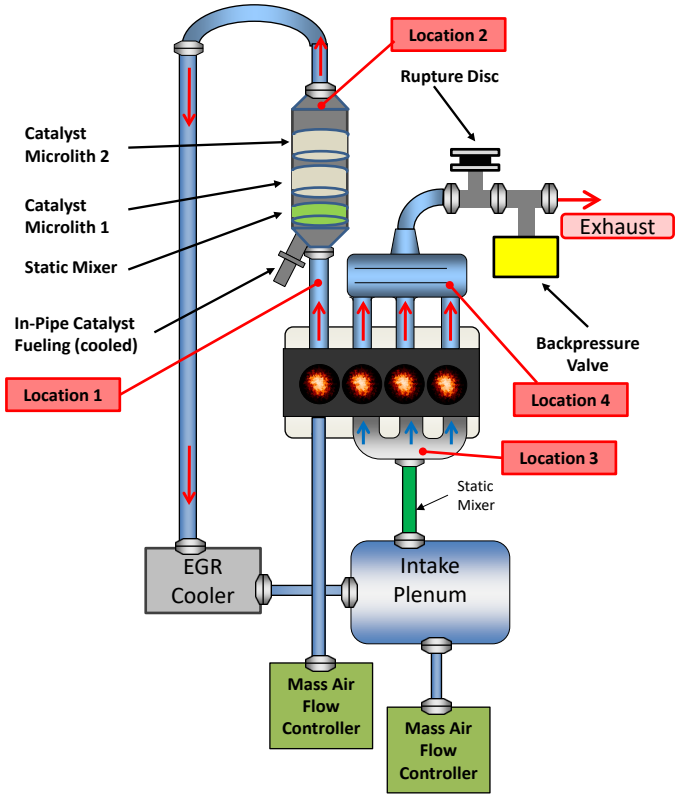

Figure 1. Schematic of modified engine system configuration with isolated cylinder for catalytic reforming. Figure adapted from our prior work, Szybist et al. [4]. The four locations noted are discussed in the Results section.

The exhaust for cylinder 4 was configured with an in-pipe fueling system to provide fuel to the catalyst. This was accomplished using a Bosch port fuel injection (PFI) injector (part number 0 280 158 123) with a static flow rate of 613 cc/min at 3.8 bar for gasoline, and a gaseous Bosch PFI injector (part number 0 280 158 821) which was designed for natural gas, for LPG. Note that for the DI fueling, liquid phase LPG was used with the DI fueling system, but due to the lower pressure of the PFI system (5 bar), it was necessary to use gaseous LPG for catalyst fueling. Gaseous LPG was taken from the vapor port from the same tank supplying the liquid LPG, sending that flow through the second Micromotion CMF010 Coriolis flow meter, then regulating the pressure down from the tank pressure of 8-10 bar to 5 bar for the gaseous PFI fuel injector.

In both cases, the PFI fuel injector was housed inside a water-cooled housing from the urea doser for a Cummins ISX15 heavy-duty diesel engine. The urea doser on the Cummins ISX15 also uses the same injector form factor but has a lower flow rate than the PFI injector used in this study, thus no modifications to the water-cooled injector housing were necessary. The fuel injector and housing assembly, prior to installing the exhaust insulation, is shown in Figure 2.

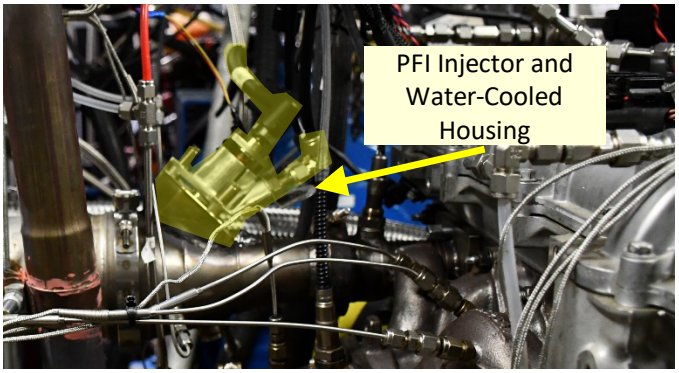

Figure 2. Water-cooled PFI injector mounted in the exhaust of cylinder 4 to provide the in-pipe catalyst fueling. Figure was originally shown in our prior work (Szybist et al. [4]).

The PFI injector sprays onto a static mixer intended to minimize fuel and air inhomogeneities upstream of the catalyst. This consists of three layers of perforated stainless steel 0.25 in thick, 0.25 in hole size, 40% open area with a staggered hole arrangement). The static mixer was fabricated in-house to provide a tortuous path to assist mixing, but the performance of the mixer was not quantified. A picture of the static mixer was shown in our previous publication [4].

Two sections of a metal-supported Microlith® reforming catalyst, developed by Precision Combustion, Inc. (PCI), were used in this investigation. Microlith reforming catalysts have been reported in other configurations in the past [49, 50], but this is the first time they are being applied to this type of EGR loop. Each 7.9 mm (0.312") long catalyst section is installed in an exhaust pipe with a diameter of 101.9 mm (4"). Each catalyst section had a platinum group metal (PGM) based reforming catalyst loading of 1.035 g, for a total reforming catalyst loading of 2.07g. The location of the reforming catalysts can be seen in the engine schematic in Figure 1, and a photograph of the reforming catalyst sections prior to installation can be seen in Figure 3.

Figure 3. Picture of the Microlith® reforming sections, developed by PCI, prior to installation in the engine. Also seen in the photograph are the thermocouples and gas sampling probes located at the catalyst-out position.

In order to make the reforming process as thermodynamically efficient as possible, minimizing heat losses upstream of and within the reforming catalyst sections is critical. To minimize heat losses, the exhaust and catalyst sections for cylinder 4 were insulated using a high-temperature 2" thick mineral wool with an R-value of 8.7. The insulation was then jacketed with corrugated aluminum.

Pressure-compensated wideband oxygen sensors were used to monitor the gas composition at four points in the system. The sensors consisted of Bosch LSU 4.2 sensors packaged with CAN communication modules from ECM. The four positions that were monitored were 1) cylinder 4 outlet prior to the in-pipe fuel injection, 2) reforming catalyst outlet, 3) intake manifold, and 4) the combined engine exhaust, as indicated in Figure 1.

A series of gas analyzers (described below) were used to monitor the mixture composition at the same 4 points in the system as the wideband oxygen sensors with one exception: the cylinder 4 composition was measured downstream of the in-pipe fuel injection instead of upstream due to space constraints. The sampling points were changed using a heated electromechanical 5-way valve from Hoke (model 0172L2P). All locations were sampled using sample lines and filters heated to 190 °C. Emissions analyzers consisted of a California Analytical 602P, which includes near infrared CO and CO_2 analyzers as well as a paramagnetic O_2 analyzer, and a California Analytical 604 flame ionization detector to measure total hydrocarbons. For the conventional combustion baseline conditions, a California Analytical series 600 HCLD analyzer was used to measure NOx emissions, but this was taken offline for the reforming conditions, where NH_3 could be present at some of the sampling points, which can then form ammonium nitrate crystals in the presence of ozone in the analyzer. Instead, for the reforming conditions, concentrations of water, CO_2, CO, CH_4, NO, NO_2, NH_3, acetylene, ethylene, ethane, and methane were measured using a MultiGas 2030HS Fourier transform infrared (FTIR) instrument from MKS Instruments. Hydrogen was measured using an Omnistar quadrupole mass spectrometer system from Pfeiffer Vacuum.

Results

This section is divided into 4 sub-sections. The first provides a performance comparison of gasoline and LPG in the conventional SI configuration. The second provides details to conceptualize the composition at the various locations throughout the system for the EGR-loop reforming operation, while the third sub-section presents engine performance for the EGR-loop reforming for both gasoline and LPG under the production r_c configuration. The last sub-section presents results for EGR-loop reforming at the high r_c configuration.

Conventional Gasoline and LPG Performance

This sub-section presents the engine performance for conventional SI operation with gasoline and LPG to serve as a baseline for comparison for the EGR-loop reforming operation. The brake thermal efficiency (BTE) as a function of engine speed and load is shown as a contour plot for gasoline in Figure 4. BTE increases as a function of engine load. Below 10 bar BMEP, there is little dependence on engine speed. For engine loads above 10 bar BMEP, BTE increases with engine speed. This can be attributed to engine knock at the high load and low speed conditions and is illustrated in Figure 4 with iso-lines showing the knock-limited CA50 combustion phasing is as late as 24 CAD $aTDC_f$. Retarding combustion phasing to avoid knock is effective, but it results in a lower efficiency because there is lower utilization of the expansion stroke, as explained in our prior work (Szybist and West [51]).

Figure 5 shows a comparison of BTE for gasoline and LPG at each of the three speeds investigated. The largest difference between these two fuels is at the high load and low speed operating conditions (12 bar BMEP and higher at 1,500 rpm, and 14 bar BMEP and higher at 2,000 rpm). At these conditions with LPG, none of the engine operating points are knock-limited, thus retarded combustion phasing is not required. Under knock-limited phasing, the BTE for the

gasoline fuel is as much as 4 BTE percentage points lower than for the LPG.

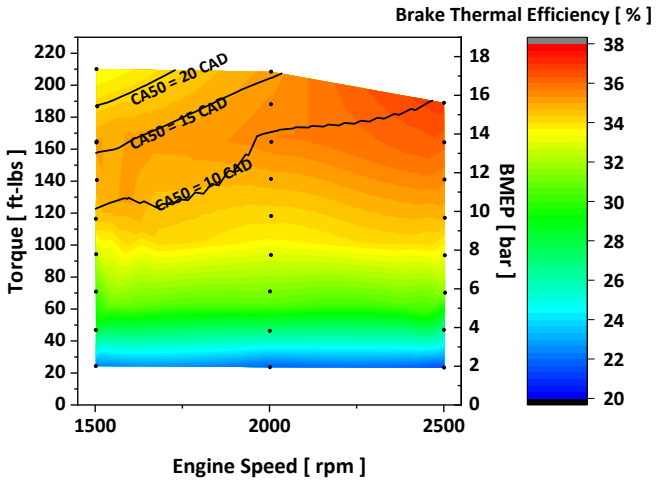

Figure 4. BTE as a function of engine speed and engine load for gasoline under the conventional SI operating conditions. CA50 iso-lines indicate knock-limited combustion phasing.

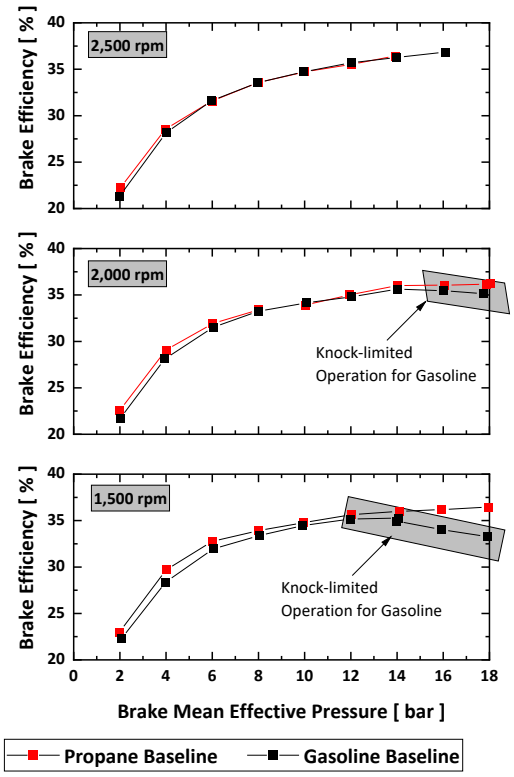

Figure 5. BTE as a function of engine load for the three different engine speeds investigated for gasoline and LPG under the conventional SI operating conditions.

The exhaust stroke utilization (ESU) metric, shown in equation 6, is a useful way to illustrate the potential for efficiency based on both combustion phasing and combustion duration:

$$ESU = \frac{\sum_{\theta=CA05}^{\theta=CA95} \dot{Q}_{HR}(\theta) * r_c(\theta)}{\sum_{\theta=CA05}^{\theta=CA95} \dot{Q}_{HR}(\theta) * r_c} \quad (6)$$

where θ is the crank angle, CA05 and CA95 represent the 5% and 95% mass fractions burned, respectively, and $\dot{Q}_{HR}$ is the rate of heat release. This equation is based on the methodology by Northrop et al. [52], but has been normalized for r_c and has been used previously by Dal Forno Chuahy et al. [53].

The ESU for the gasoline at the baseline configuration is shown in Figure 6. The LPG results are not shown here for brevity but were found to be qualitatively similar to gasoline with the exception that there is not a decrease in ESU at the high load and low speed operating conditions. This ESU decrease occurs under the knock-limited phasing operating conditions for gasoline, which are illustrated in Figure 4 and Figure 5. It is also noteworthy that there is not a significant decrease in ESU at the lightest load conditions, which stands in contrast to the reforming operating conditions as will be discussed later.

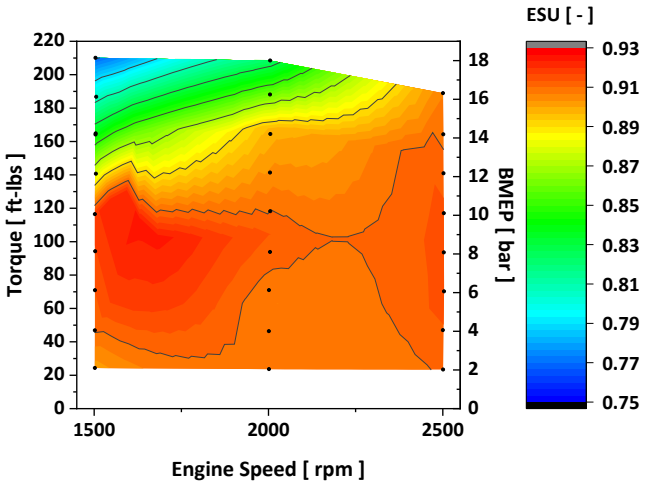

Figure 6. ESU as a function of engine speed and engine load for gasoline under the conventional SI operating conditions.

EGR-Loop Reforming Conceptualization

The EGR-loop reforming configuration is a significant departure from conventional engine operation where all engine cylinders are subjected to the same nominal boundary conditions and perform the same nominal task. To assist in the conceptualization of this, the schematic in Figure 1 includes labels for locations 1 – 4. The temperature and select compositions are provided in Table 4. For illustration purposes, compositions from the 2,000 rpm, 8 bar BMEP operating point are listed and discussed here. However, these are meant to be qualitatively representative for most of the operating map. Observations are as follows:

- Location 1: This is the engine-out location from cylinder 4, which operates fuel lean and feeds the reforming catalyst. The fuel-lean condition results in both the presence of nearly 2% O_2 and a very high NOx concentration. H_2 and NH_3 concentrations are both negligible at this location, and the CO concentration of approximately 1,000 ppm is a

factor of 4-5 lower than would be expected for stoichiometric combustion.

- Location 2: This is the reforming catalyst-out location and represents the condition of the exhaust after fuel has been added to the composition noted in Location 1 and reformed over the PGM-based catalyst. At this location, the H_2 and CO concentrations are both over 3%, but H_2 and CO concentrations at this location are highly dependent on engine speed and load as is illustrated later. It can also be seen that the oxidizers from Location 1 (O_2 and NOx) are completely consumed during the reforming process. Additionally, nearly half of the NOx present at Location 1 is converted to NH_3 over the reforming catalyst.
- Location 3: This is the intake manifold after the reformate from Location 2 has been mixed with fresh air. This shows that the inlet O_2 concentration is 14.6%, which equates to just over 30 vol% EGR. The H_2, NH_3, and CO concentrations have all been reduced proportionally relative to Location 2 due to dilution with fresh air.
- Location 4: The exhaust manifold is under stoichiometric conditions and is compatible with a conventional TWC emission control catalyst. The concentrations of H_2, CO, and O_2 are typical for a stoichiometric engine. The concentration of NOx in the exhaust is comparable to the concentration of NH_3 in the intake, indicating that this is the primary source of NOx in the exhaust, rather than thermal NOx during combustion. This is consistent with our observations in previous work (Chang and Szybist [11]) where we showed that NOx emissions could be decreased to less than 100 ppm with 25% EGR. While this level of NOx emissions does require treatment with a TWC emission control catalyst, it is worth noting that this does represent a factor of 4-6 decrease from non-dilute SI combustion at this operating condition.

Table 4. Temperature and select species concentrations at 4 locations for EGR loop operation at 2,000 rpm, 8 bar BMEP. The four locations are shown in Figure 1.

	Location 1: Cyl. 4 Out	Location 2: Reforming Cat Out	Location 3: Intake Manifold	Location 4: Exhaust Manifold
T [°C]	637	595	39	555
O_2 [%]	1.90	0.00	14.60	0.61
CO [%]	0.11	3.23	1.00	0.48
H_2 [%]	0.00	3.83	0.89	0.10
NOx [ppm]	3,800	0	0	540
NH_3 [ppm]	0	1600	500	9

Reforming Configuration Brake Thermal Efficiency

The engine was operated in a reforming configuration for both gasoline and LPG from 2-14 bar BMEP across the same engine speed range investigated in the baseline configuration, 1,500-2,500 rpm. The peak operable loads for this engine were limited relative to the baseline configuration to remain below the rated pressure of the intake and exhaust system (2.2 bar absolute). A contour plot showing the BTE for gasoline as a function of speed and load is shown in Figure 7. Similar to Figure 4, Figure 7 shows iso-lines of the knock-limited CA50 combustion phasing. However, this only represents the cylinder 4 combustion phasing, which is the cylinder operating fuel-lean and feeding the reforming catalyst. The remaining cylinders that are operating with the EGR/reformate mixture are not knock-limited. Thus, while there is some decrease in efficiency that is experienced when only cylinder 4 becomes knock-limited, it is not as severe as was shown in Figure 4.

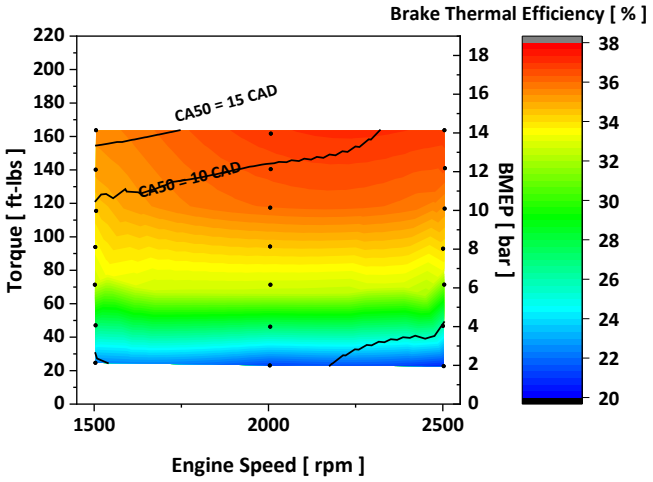

Figure 7. BTE as a function of engine speed and engine load for gasoline under the conventional SI operating conditions. CA50 iso-lines indicate knock-limited combustion phasing for cylinder 4. Cylinders 1-3 were not knock-limited.

Figure 8 compares BTE for gasoline under the conventional baseline operating conditions and under the reforming conditions, and Figure 9 shows the same comparison for LPG. For both fuels, the largest BTE benefits for the reforming strategy are realized at 2,000 and 2,500 rpm, and at loads between 4 and 12 bar BMEP. In this range, BTE increased by as much as 1.85 percentage points, corresponding to more than a 5% relative increase in efficiency

It is notable that for both fuels, there are minimal efficiency benefits at the lightest load condition of 2 bar BMEP, or in some cases, a reduction in efficiency. The intake manifold pressure for conventional operation and the reforming strategy can be seen in Figure 10 as a function of engine load at 2,000 rpm (which is representative of all three engine speeds investigated). The relationship between intake manifold pressure and load is nearly linear for the reforming strategy but is decidedly non-linear for the conventional operation, which reflects the cam phasing strategies employed. For the reforming strategy, a fixed cam position was used at all conditions to minimize the in-cylinder trapped residuals. Due to the very high dilution levels were already present with the EGR-loop reforming strategy, further trapped residual induced with cam phasing strategies was undesirable from a stability standpoint. In contrast, the conventional SI baseline employed a cam phasing strategy that minimized pumping work at lighter loads by increasing the trapped residuals and decreasing the trapped swept volume. As a result, there are only minimal differences in the intake manifold pressure between the conventional and reforming strategies at the two lightest-load conditions.

The final observation regarding BTE differences between conventional and the reforming operation, shown in Figure 8 and Figure 9, is that the BTE benefit at 1,500 rpm is smaller than at the 2,000 and 2,500 rpm engine speeds. More specifically, at engine loads 10 bar and higher, there is no BTE benefit for the reforming operation. We are attributing the reduced benefit at 1,500 rpm to air handling requirements. Figure 10 shows that boosted operation for the reforming strategy is required by 8 bar BMEP. As described in the methodology section, backpressure is applied during boosted operation to the engine to hold the combined turbocharger efficiency

to 40% using the methodology by Trenc et al.[47], which considers the exhaust flowrate, temperature, and pressure.

Figure 11 shows the exhaust temperatures achieved for gasoline at both the conventional SI and EGR loop reforming strategies. The EGR-loop reforming strategy produces an exhaust temperature that is up to 130 °C lower than conventional SI operation. For air handling purposes, this necessitates a higher backpressure and more pumping work than conventional SI. The net effect of the need for backpressure and the low temperature exhaust can be seen in the pumping mean effective pressure (PMEP), Figure 12. For the reforming strategy there is a minimum in pumping work (maximum PMEP value) at 8 bar BMEP, and at higher loads the need for increased backpressure causes the pumping work to increase. While this trend is true at all speeds, only the 1,500 rpm engine speed exhibits a crossover where the reforming strategy actually requires more pumping work than conventional SI, which can be attributed to this speed having the lowest temperatures, as shown in Figure 11.

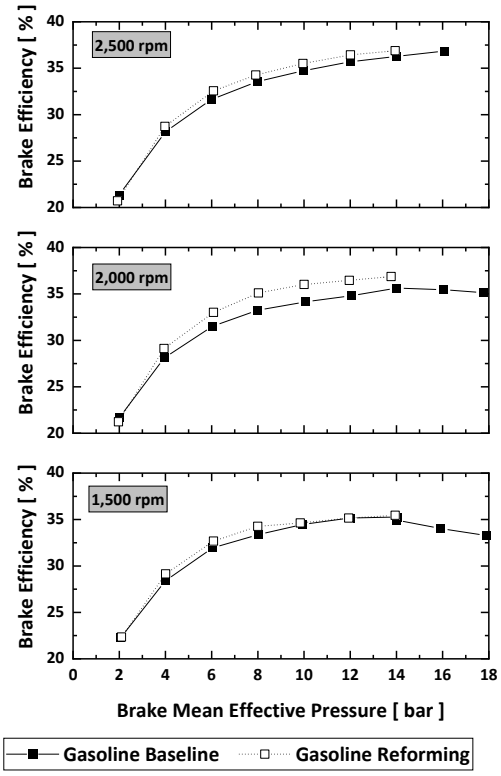

Figure 8. BTE as a function of engine load for the three different engine speeds investigated for gasoline under the conventional baseline conditions and under the EGR-loop reforming conditions.

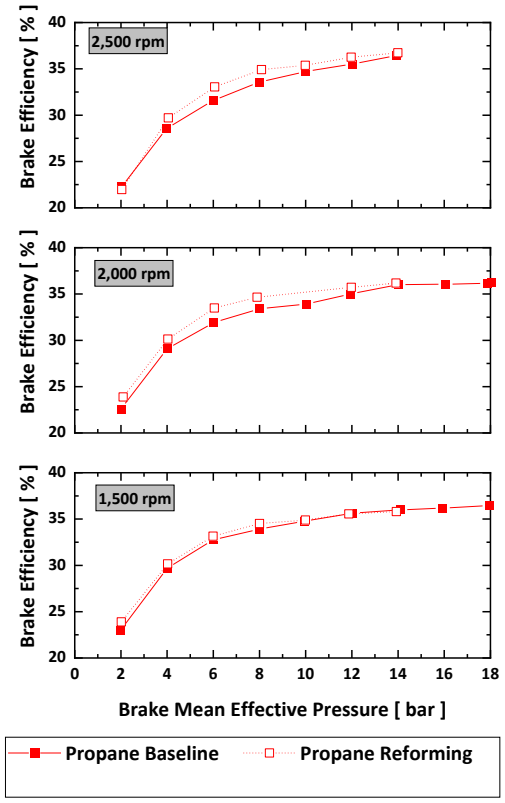

Figure 9. BTE as a function of engine load for the three different engine speeds investigated for gasoline under the conventional baseline conditions and under the EGR-loop reforming conditions.

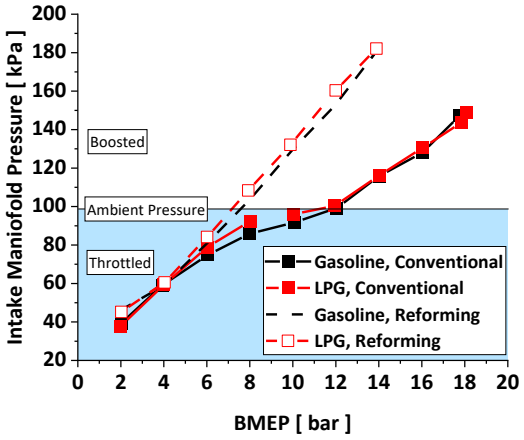

Figure 10. Intake manifold pressure as a function of engine load at 2,000 rpm for gasoline and LPG under conventional and reforming configurations.

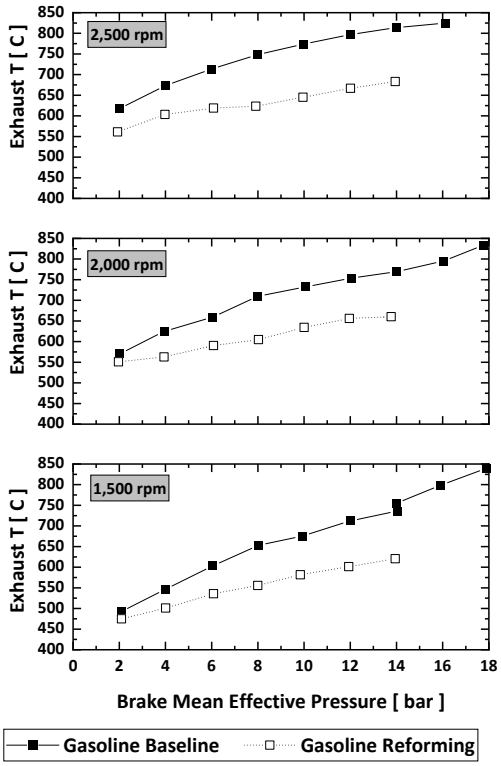

Figure 11. Exhaust temperature as a function of engine load for gasoline under both the conventional SI and EGR-loop reforming strategies at each of the engine speeds investigated.

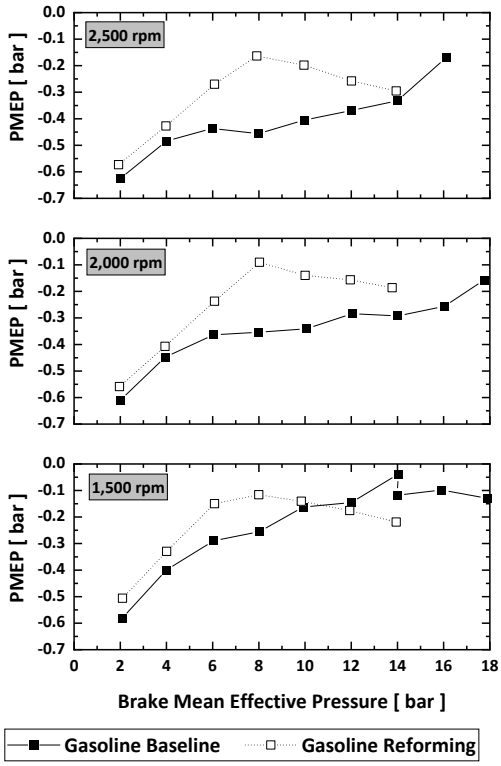

Figure 12. PMEP as a function of engine load for the three different engine speeds investigated for gasoline under the conventional baseline conditions and under the EGR-loop reforming conditions.

To provide further insight into the differences between the conventional and reforming operation, Figure 13 provides a comparison of in-cylinder pressure and heat release rate for three different engine speed and load operating conditions: 1,500 rpm and 4 bar BMEP; 2,000 rpm and 10 bar BMEP, and 2,500 rpm and 14 bar BMEP. While these operating conditions span a wide range of power levels, similar observations can be made from all three:

The first observation is that there is higher pressure during the compression stroke for the EGR-loop reforming operation, which can be attributed to the additional mass and higher intake manifold pressure from the high levels of EGR dilution. This difference is relatively small for the 4 bar BMEP condition, due to the small difference in intake manifold pressure at the lightest loads as was shown in Figure 10. Nonetheless, it is present for all conditions and the difference increases at the higher speeds and loads.

The second observation from Figure 13 is that the combustion event is elongated, with combustion for the EGR dilution strategy starting earlier and ending later than the conventional SI combustion. This includes a very slow flame kernel development process for the reforming conditions, as is illustrated by the much earlier spark timing conditions for the reforming strategy. The elongated combustion process is consistent with our prior work [4] and can be attributed to a slower flame speed at these highly dilute conditions, despite the presence of reformed products.

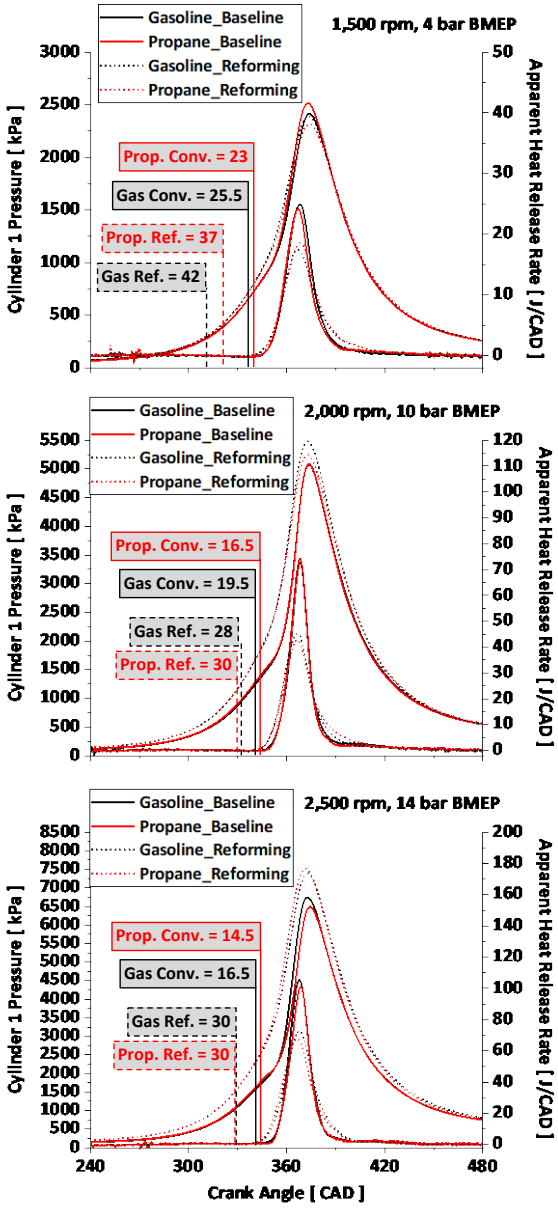

Figure 13. Cylinder pressure and heat release rate for three speed/load operating conditions comparing the baseline and EGR-loop reforming and the fuel type. Labels indicate spark timing in CA deg bTDC$_f$.

The elongation of the combustion process is undesirable and decreases efficiency because it is further from the ideal Otto cycle, which assumes a constant volume heat addition [54]. Just as ESU can be used to illustrate non-idealities with combustion phasing to prevent knock, it can be used to illustrate non-idealities due to combustion duration. The ESU for reforming operation is shown in Figure 14 for gasoline and in Figure 15 for LPG, where values range from less than 0.8 to a maximum of about 0.9. This is a significant reduction compared to conventional SI, which achieved an ESU of about 0.93 over the entire operating map except for where it was knock-limited, as was shown in Figure 6. Further, the reforming operating mode experiences a significant decrease in ESU at the lightest load conditions whereas conventional operation does not. It is notable that there is a more severe ESU decrease for gasoline than with LPG, which will be discussed further in the context of H_2 production. The decrease in ESU at the lightest load conditions is an additional reason why there wasn't an efficiency benefit to the reforming strategy at the lightest load, as was shown in Figure 8 and Figure 9.

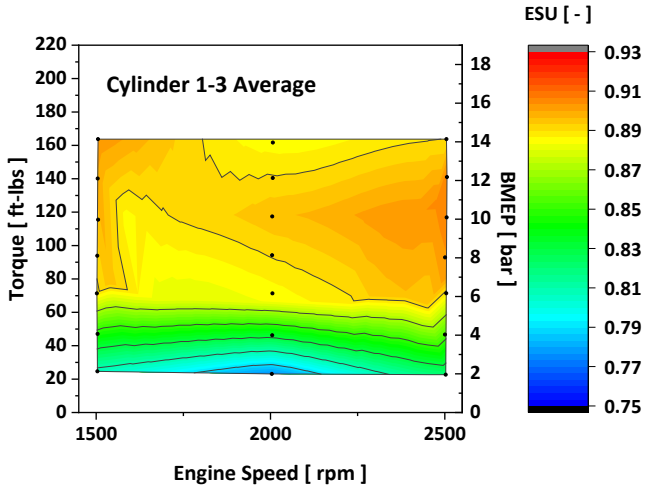

Figure 14. ESU as a function of engine speed and engine load for cylinders 1-3 using gasoline under the EGR loop reforming configuration.

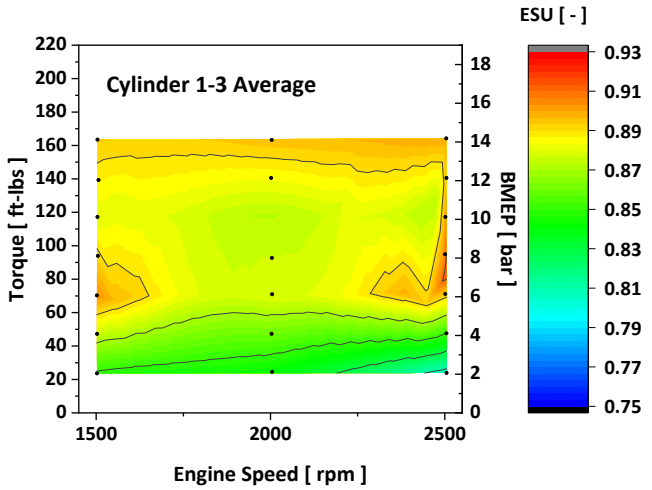

Figure 15. ESU as a function of engine speed and engine load for cylinders 1-3 using LPG under the EGR loop reforming configuration.

As was noted in the Introduction and Methodology sections, the boundary conditions for the reforming catalyst were held constant at a catalyst inlet O_2 concentration of 2.0 ± 0.2%, and catalyst Φ of 8.0 ± 1.0. Under these conditions, the reforming catalyst produced H_2 at levels of 2.1 to 10.4% for gasoline, resulting in intake manifold H_2 levels of 0.6 to 2.9%, as shown in Figure 16. The H_2 production increases with both engine speed and engine load, similar to the trends in exhaust temperature shown in Figure 11. Interestingly, there are significant differences in the intake manifold H_2 for the LPG fuel, as shown in Figure 17. Unlike gasoline, the H_2 concentrations for LPG do not decrease as significantly at the low speed and low load conditions. The intake manifold H_2 being higher at the lightest load conditions is consistent with the ESU results shown in Figure 14 and Figure 15, where LPG exhibited a higher ESU than gasoline at the lightest loads. However, the peak H_2 concentrations for LPG are comparable to or lower than the H_2 concentrations for gasoline. One of the motivations for investigating

LPG for this reforming strategy was that it has a higher H/C than gasoline, and we theorized that this would produce higher H_2 levels. This result shows that H_2 production is not universally higher for LPG than for gasoline, but that LPG reforming appears to be most beneficial at lightest load conditions despite the two fuels having nominally the same temperature at the catalyst inlet.

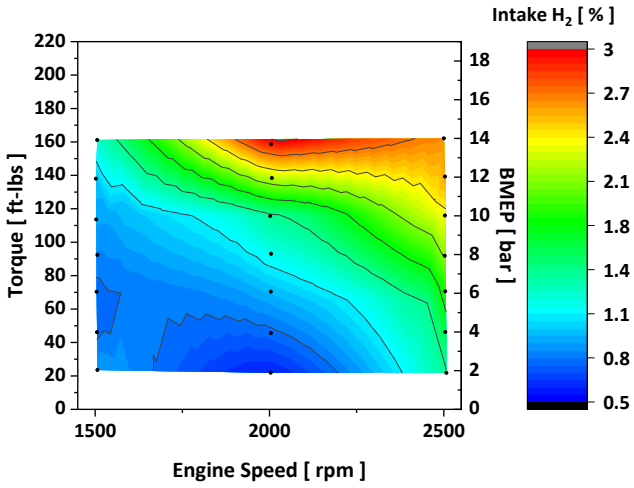

Figure 16. Intake manifold H_2 concentration under EGR loop reforming conditions for gasoline.

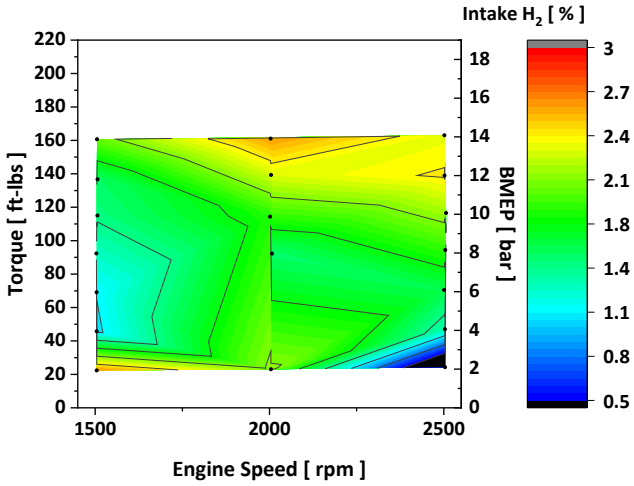

Figure 17. Intake manifold H_2 concentration under EGR loop reforming conditions for LPG.

High Compression Ratio Reforming

The final results sub-section presents a higher r_c for cylinders 1-3 to take advantage of the increased knock resistance with high dilution and fuel reforming. The improved knock resistance with the reformate mixture was confirmed, with only one operating condition exhibiting knock in the reforming cylinders, at 1,500 rpm and 14 bar BMEP. At this condition, CA50 combustion phasing had to be retarded from the optimal phasing of 8 to 12 CA deg aTDC$_f$, which is a very modest retard of combustion phasing.

Figure 18 shows BTE as a function of load for the conventional SI baseline, EGR-loop reforming at the stock compression ratio, and EGR-loop reforming at the higher r_c of 11.85:1 for cylinders 1-3, which are the cylinders consuming the reformate. It can be seen that the higher r_c does provide efficiency benefits at all engine speeds, including increasing the peak efficiency to a value of 38.2% from the baseline SI peak value of 36.6%. However, the efficiency gains with the high r_c were modest under most operating conditions.

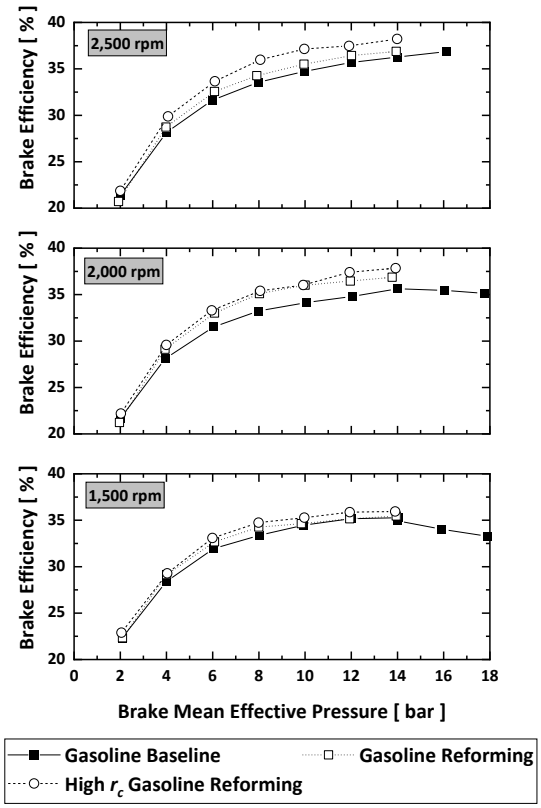

Figure 18. BTE as a function of engine load for conventional SI, EGR-loop reforming at the stock compression ratio, and EGR loop reforming at a higher compression ratio of 11.85. for gasoline.

Examining the cylinder pressure and heat release rate for the high r_c EGR loop reforming, as shown in Figure 19 for the 2,000 rpm and 10 bar BMEP condition, can provide additional insight into why the efficiency gains were modest. It can be seen that the higher r_c produced a higher cylinder pressure, such that the peak cylinder pressure is nearly 70 bar compared to only around 50 bar for the gasoline baseline operation at the same load. It can also be seen that the heat release rate is even further attenuated relative to the stock r_c EGR loop reforming operation.

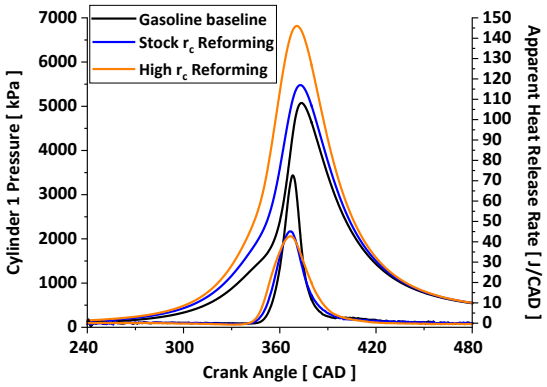

Figure 19. Cylinder pressure and heat release rate at 2,000 rpm and 10 bar BMEP for gasoline baseline SI operation, stock r_c EGR loop reforming, and high r_c EGR loop reforming.

This attenuated heat release rate can be quantified as part of the ESU calculation, shown in Figure 20. It was found that moving to a higher r_c produced an additional ESU reduction throughout the load range except for the lightest engine load which already had a very low ESU. Keeping the fast-burn characteristics of a combustion chamber when moving to a higher r_c is a well-known challenge with SI engines, and to overcome this, many high r_c concepts are moving towards an engine geometry with a higher stroke-to-bore ratio to maintain clearances in the combustion chamber for proper flame kernel development [55]. The results from this study indicate that the high r_c combustion chamber was not as conducive to fast combustion as the stock combustion chamber, despite the presence of H_2 in the combustion chamber.

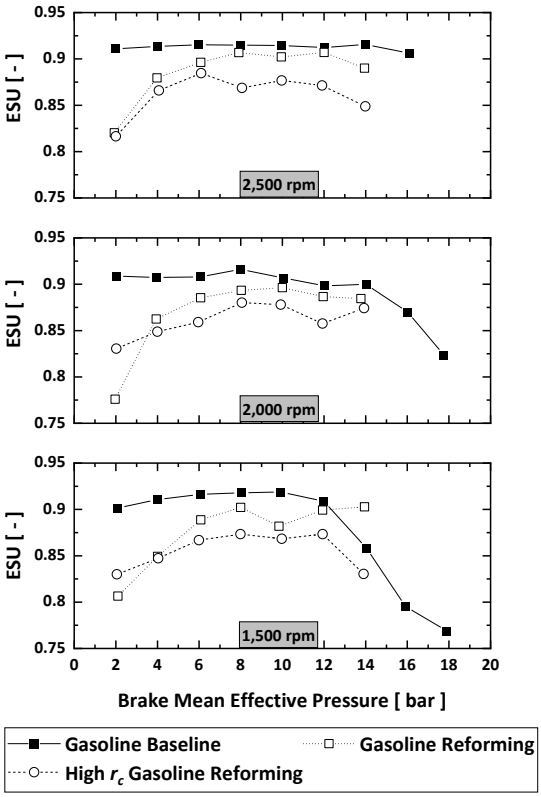

Figure 20. ESU as a function of engine load for conventional SI, EGR-loop reforming at the stock compression ratio, and EGR loop reforming at a higher compression ratio of 11.85. for gasoline.

Post-testing observations concerning the Microlith®-based reforming catalyst

Upon conclusion of the performance experiments described in the previous sub-sections, the Microlith®-based catalyst was removed and examined. Figure 21 shows a photograph of the catalyst assemblies after approximately 100 hours on-stream. The catalyst survived well with minor spalling. The majority of the spalling was observed at the edges, presumably due to increased compression from packaging. Red deposits (presumably rust) were observed at the inlet of the catalyst bed.

Figure 21. Photograph of the Microlith®-based reforming catalyst cylinders after approximately 100 hours of testing.

Discussion

The discussion section is structured to reflect on the three objectives for this investigation stated at the end of the introduction section: 1) determine if a higher H/C fuel like LPG provides a reforming benefit, 2) expand the speed-load range for the EGR-loop operation, and 3) take advantage of the higher knock resistance of the dilute mixture with reformate to increase efficiency.

Use of LPG for EGR-Loop Reforming

It was theorized that the higher H/C of propane, which is the primary constituent of LPG, had the potential to produce higher H_2 yields under reforming conditions and improve the thermodynamics of the reforming process. However, the results showed this was not the case across the full operating map, and in fact, the highest H_2 concentrations were observed for gasoline. A benefit for LPG was observed under the lighter load and lower speed operating conditions when the H_2 production for gasoline was lowest. At these conditions, the H_2 production for LPG did not decrease as significantly as it did for gasoline under low temperature conditions. The reason for this result isn't clear, but there is ongoing work at ORNL with a synthetic exhaust flow reactor experiment that will provide further insights and will be the subject of a future publication.

Range of Operation for EGR-Loop Reforming

It was successfully demonstrated that the speed and load range could be expanded over a wide range of operating conditions while also producing an efficiency benefit. The efficiency gains were low and inconsistent at the lightest load operating condition but were also negligible at high loads at 1,500 rpm, which is attributed to air handling penalties. This observation illustrates that this reforming strategy can be applicable over a wide range of reformer space velocity and temperature conditions.

Furthermore, this work illustrated that this reforming strategy is compatible with the metal-supported Microlith catalyst from PCI. Our previous work used ceramic monolith technology, which had a significantly higher volume than the metal-supported Microlith catalyst, and takes significantly longer to heat up and respond to changing conditions due to its higher mass. The Microlith-based technology was advantageous in that it could be more easily packaged into a vehicle and provide faster heat up during operating transients.

Improved Efficiency Potential

This work illustrated that, while the EGR-loop reforming strategy did increase efficiency, there was a tradeoff where a reduction in ESU due to slower combustion was countering the efficiency improvements. Furthermore, this study also showed that the EGR-reformate mixture was successful at mitigating knock and allowing for operation at higher r_c. The knock mitigation potential, however, wasn't fully realized because of further ESU decreases at the higher r_c.

As a result, it will be crucial to incorporate additional engine technologies to fully realize the potential of EGR-loop reforming. Specifically, advanced ignition technologies that can speed up combustion, such as prechambers, which have been shown to reduce combustion duration under dilute conditions, may be helpful in minimizing the ESU penalty with the EGR-loop reforming strategy. Additionally, shifting to a higher stroke-to-bore ratio should allow the compression ratio to be increased without compromising the combustion chamber clearance volumes. This should facilitate flame kernel development, and also increase the mean piston speed which increases turbulence for faster combustion [55].

Conclusions

In this investigation, the EGR-loop reforming strategy was extended from prior work in multiple respects. First, it was extended to the Microlith® metal-supported reforming catalyst from PCI, which provides significant benefits in catalyst warm-up and packaging relative to ceramic monolith catalysts. Second, the engine operating range was expanded to include a speed range of 1,500 to 2,500 rpm and a load range of 2 to 14 bar BMEP. Next, the impact of the H/C of the fuel was investigated by comparing LPG to gasoline. Finally, the knock mitigation benefits of the EGR reformate mixture was investigated by increasing the r_c of the cylinders consuming the dilute EGR reformate mixture. The following conclusions can be made from this investigation:

- The Microlith® metal-supported reforming catalyst from PCI provides robust performance across a wide range in inlet temperature and space velocity, corresponding to the expanded engine speed and load operating range. The catalyst did not show significant degradation after approximately 100 hours on-stream.
- Efficiency benefits were observed across the majority of the expanded speed and load range, and exceeded a 5% relative efficiency improvement. The exceptions to this were at the lightest load investigated (2 bar BMEP), which is attributed to a very long combustion duration, and at high loads at 1,500 rpm, which is attributed to high pumping work.
- The high H/C of the LPG did not provide universal increased H_2 yields relative to gasoline across the operating map. Some higher H_2 yields were observed at the lightest operating loads, but at the higher loads where the catalyst inlet temperature was higher, the H_2 yields for gasoline were higher than for LPG.
- Experimental results illustrated that there was a knock mitigation benefit of the EGR reformate mixture. For the cylinders consuming this dilute mixture, no conditions were knock-limited at the stock r_c of 9.2, and only one condition was knock-limited at the higher r_c of 11.85.
- Despite the improved knock resistance, only minor efficiency benefits were realized because of the lower ESU with the dilute combustion strategy. However, results illustrate that additional efficiency benefits could be realized if the combustion duration could be reduced.

References

[1] Chang Y, Szybist JP, Pihl JA, Brookshear DW. Catalytic Exhaust Gas Recirculation-Loop Reforming for High Efficiency in a Stoichiometric Spark-Ignited Engine through Thermochemical Recuperation and Dilution Limit Extension, Part 1: Catalyst Performance. Energ Fuel. 2018;32:2245-56.
[2] Chang Y, Szybist JP, Pihl JA, Brookshear DW. Catalytic Exhaust Gas Recirculation-Loop Reforming for High Efficiency in a Stoichiometric Spark-Ignited Engine through Thermochemical

Recuperation and Dilution Limit Extension, Part 2: Engine Performance. Energ Fuel. 2018;32:2257-66.
[3] Brookshear DW, Pihl JA, Szybist JP. Catalytic Steam and Partial Oxidation Reforming of Liquid Fuels for Application in Improving the Efficiency of Internal Combustion Engines. Energ Fuel. 2018;32:2267-81.
[4] Szybist JP, Pihl J, Huff S, Kaul B. High Load Expansion of Catalytic EGR-Loop Reforming under Stoichiometric Conditions for Increased Efficiency in Spark Ignition Engines. SAE Int. J. Adv. & Curr. Prac. in Mobility 2019;1(2):588-600.
[5] Splitter DA, Pawlowski AE, Wagner RM. A Historical Analysis of the Co-evolution of Gasoline Octane Number and Spark-Ignition Engines. Front Mech Eng. 2016;1:1-22.
[6] Alger T, Chauvet T, Dimitrova Z. Synergies between High EGR Operation and GDI Systems. SAE International Journal of Engines. 2008;1:101-14.
[7] Caton JA. A Comparison of Lean Operation and Exhaust Gas Recirculation: Thermodynamic Reasons for the Increases of Efficiency. SAE Technical Paper 2013-01-0266; 2013.
[8] Alger T, Mangold B, Roberts C, Gingrich J. The Interaction of Fuel Anti-Knock Index and Cooled EGR on Engine Performance and Efficiency. SAE International Journal of Engines. 2012;5:1229-41.
[9] Szybist JP, Splitter D. Effects of Fuel Composition on EGR Dilution Tolerance in Spark Ignited Engines. Sae International Journal of Engines. 2016;9:819-31.
[10] Szybist J. Knock Mitigation Effectiveness of EGR across the Pressure-Temperature Domain. SAE International Journal of Advances and Current Practices in Mobility. 2020;3:262-75.
[11] Chang Y, Szybist JP. Fuel Effects on Combustion with EGR Dilution in Spark Ignited Engines. The 2016 Spring Technical Meeting of the Central States Section of the Combustion Institute (CSSCI 2016). Knoxville, TN: CCSI 145IC-0082; 2016.
[12] Tabata M, Yamamoto T, Fukube T. Improving NOx and Fuel Economy for Mixture Injected SI Engine with EGR. SAE Technical Paper 950684, 1995.
[13] Cairns A, Blaxill H, Irlam G. Exhaust Gas Recirculation for Improved Part and Full Load Fuel Economy in a Turbocharged Gasoline Engine. SAE Technical Paper 2006-01-0047, 2006.
[14] Kaul BC, Finney CEA, Wagner RM, Edwards ML. Effects of External EGR Loop on Cycle-to-Cycle Dynamics of Dilute SI Combustion. SAE Technical Paper 2014-01-1236, 2014.
[15] Duchaussoy Y, Lefebvre A, Bonetto R. Dilution Interest on Turbocharged SI Engine Combustion. SAE Technical Paper 2003-01-0629, 2003.
[16] Martz JB, Middleton RJ, Lavoie GA, Babajimopoulos A, Assanis DN. A computational study and correlation of premixed isooctane-air laminar reaction front properties under spark ignited and spark assisted compression ignition engine conditions. Combust Flame. 2011;158:1089-96.
[17] Stone CR, Brown AG, Beckwith P. Cycle-by-Cycle Variations in Spark Ignition Engine Combustion - Part II: Modelling of Flame Kernel Displacements as a Cause of Cycle-by-Cycle Variations. SAE Technical Paper 960613, 1996.
[18] Conte, E. and Boulouchos, K., Hydrogen-enhanced gasoline stratified combustion in SI-DI engines. Journal of Engineering for Gas Turbines and Power-Transactions. 2008;130.
[19] Ji, C.W. and Wang, S.F., Effect of hydrogen addition on combustion and emissions performance of a spark ignition gasoline engine at lean conditions. International Journal of Hydrogen Energy. 2009;34:7823-34.
[20] D'Andrea, T., Henshaw, P., and Ting, D.S.K., The addition of hydrogen to a gasoline-fuelled SI engine. International Journal of Hydrogen Energy. 2004;29:1541-52.
[21] Tahtouh, T., Halter, F., Samson, E., and Mounaïm-Rousselle, C., Effects of hydrogen addition under lean and diluted conditions on combustion characteristics and emissions in a spark-ignition engine. International Journal of Engine Research. 2011;12:466-83.
[22] Jamal Y, Wyszynski ML. On-Board Generation of Hydrogen-Rich Gaseous Fuels - A Review. Int J Hydrogen Energy. 1994;19:557-72.
[23] Fennell D, Herreros J, Tsolakis A. Improving Gasoline Direct Injection (GDI) Engine Efficiency and Emissions with Hydrogen from Exhaust Gas Fuel Reforming. Int J Hydrogen Energy. 2014;39:5153-62.
[24] Allenby S, Chang W-C, Wyszynski ML. Hydrogen Enrighment: A way to Maintain Combustion Stability in a Natural Gas Fuelled Engine with Exhaust Gas Recirculation, the Potential of Fuel Reforming. Proc Instn Mech Engrs Part D. 2001;215:405-18.
[25] Alger, T., Gingrich, J., and Mangold, B., The Effect of Hydrogen Enrichment on EGR Tolerance in Spark Ignited Engines. SAE Technical Paper. 2007:2007-01-0475, doi:10.4271/2007-01-0475.
[26] Fennell D, Herreros M, Tsolakis A, Xu H, Cockle K, Millington P. GDI Engine Performance and Emissions with Reformed Exhaust Gas Recirculation (REGR). SAE Technical Paper 2013-01-0537. 2013.
[27] Alger, T. and Mangold, B., Dedicated EGR: A New Concept in High Efficiency Engines. SAE Int J Engines. 2009;2:620-31.
[28] Alger T, Walls M, Chadwell C, Joo S, Denton B, Kleinow K, et al. The Interaction bewteen Fuel AntiKnock Index and Reformation Ratio in an Engine Equipped with Dedicated EGR. SAE Int J Engines. 9(2):786-795, 2016.
[29] Robertson D, Chadwell C, Alger T, Zuehl J, Gukelberger R, Denton B, et al. Dedicated EGR Vehicle Demonstration. SAE Int J Engines. 2017;10.
[30] Study of aOn-board Fuel Reformer and Hydrogen-Added EGR Combustion in a Gasoline Engine. SAE Int J Fuels Lubr. 2015;8:358-66, doi:10.4271/2015-01-0902.
[31] Wheeler JC, Stein R, Morgenstern D, Sall E, Taylor J. Low-Temperature Ethanol Reforming: A Multi-Cylinder Engine Demonstration. SAE Technical Paper 2011-01-0142. 2011.
[32] Integration of an E85 Reforming System into a Vehicle-Ready Package and Project Results. SAE Technical Paper. 2014:2014-01-1191, doi:10.4271/2014-01-1191.
[33] Hwang J, Li X, W. N. Exploration of Dual Fuel Diesel Engine Operation with On-Board Fuel Reforming. SAE Technical Paper 2017-01-0757. 2017.
[34] Fennell D, Herreros Arellano JM, Tsolakis A, Wyszynski M, Cockle K, Pignon J, et al. On-board Thermochemical Energy Recovery Technology for Low Carbon Clean gasoline Direct Injection Engine Powered Vehicles. Proc IMechE Part D: J Automobile Enginnering. 2017:1-13.
[35] Leung P, Tsolakis A, Rodriguez-Fernandez J, Goluski S. Raising teh Fuel Heating Value and Recovering Exhaust Heat by On-Board Oxidative Reforming of Bioethanol. Energy Environ Sci. 2010;3:780-8.
[36] Jamal Y, Wagner T, Wyszynski ML. Exhaust Gas Reforming of Gasoline at Moderate Temperatures. Int J Hydrogen Energy. 1996;21:507-19.
[37] Gomes SR, Bion N, Blanchard G, Rousseau S, Belliere-Baca V, Duprez D, et al. Thermodynamic and Experimental Studies of Catalytic Reforming of Exhaust Gas Recirculation in Gasoline Engines. Applied Catalysis B: Environmental. 2011;102:44-53.
[38] Bogarra M, Herreros JM, Tsolakis A, York APE, Millington PJ, Martos FJ. Impact of Exhaust Gas Fuel Reforming and Exhaust Gas Recirculation on Particulate Matter Morphology in Gasoline Direct Injection Engine. J Aerosol Science. 2017;103:1-14.
[39] Bogarra M, Herreros JM, Tsolakis A, York APE, Millington PJ, Martos FJ. Influence of On-Board Produced Hydrogen and Three

Way Catalyst on Soot Nanostructure in Gasoline Direct Injection Engines. Carbon. 2017;120:326-36.
[40] Golunski S. What is the Point of On-Board Fuel Reforming? Energy Environ Sci. 2010;3:1918-23.
[41] Ahmed S, Krumpelt M. Hydrogen from Hydrocarbon Fuels for Fuel Cells. Int J Hydrogen Energy. 2001;26:291-301.
[42] Chakravarthy VK, Daw CS, Pihl JA, Conklin JC. Study of the Theoretical Potential of Thermochemical Exhaust Heat Recuperation for Internal Combustion Engines. Energy & Fuels. 2010;24:1529-37.
[43] Tsolakis A, Megaritis A, Wyszynski ML. Application of Exhaust Gas Fuel Reforming in Compression Ignition Engines Fueled by Diesel and Biodiesel Fuel Mixtures. Energy & Fuels. 2003;17:1464-73.
[44] Tsolakis A, Megaritis A, Golunski SE. Reaction Profiles During Exhaust-Assisted Reforming of Diesel Engine Fuels. Energy & Fuels. 2005;19:744-52.
[45] Gomez JE, Walker B. National Propane Survey 2017-2018, Final Report. Southwest Research Institute (SwRI) for Propane Education and Research Council (PERC); 2019.
[46] Moore W, Foster M, Hoyer K. Engine Efficiency Improvements Enabled by Ethanol Fuel Blends in a GDi VVA Flex Fuel Engine. SAETechnical Paper 2011-01-0900, 2011.
[47] Trenc F, Cer M, Bizjan F, Hribernik A. Determination of the Realistic Turbocharger Efficiency with Pulsating Gas-Flow Compared on a 4-Cylinder Engine. Presented at the International Gas Turbine & Aeroengine Congress & Exhibition. Stockholm, Sweden1998.
[48] Chadwell C, Alger T, Roberts C. Boosting Simulation of High Efficiency Alternative Combustion Mode Engines. SAE Int J Engines. 2011;4:375-93.
[49] Lyubovsky M, Roychoudhury S, LaPierre R. Catalytic partial "oxidation of methane to syngas" at elevated pressures. Catalysis Letters. 2005;99:113-7.
[50] Mastanduno R, Roychoudhury S, Etemad S. Onboard Hydrogen Generation for IC Engine Emissions Reduction. ASME Internal Combustion Engine Division's 2014 Fall Technical Conference. Columbus, IN: ASME; 2014. p. ICEF2014-5627.
[51] Szybist JP, West BH. The Impact of Low Octane Hydrocarbon Blending Streams on the Knock Limit of “E85”. SAE International Journal of Fuels and Lubricants. 2013;6:44-54.
[52] Northrop WF, Fang W, Huang B. Combustion Phasing Effect on Cycle Efficiency of a Diesel Engine Using Advanced Gasoline Fumigation. J Eng Gas Turb Power. 2013;135.
[53] D.F. Chuahy F, Kokjohn SL. Effects of reformed fuel composition in “single” fuel reactivity controlled compression ignition combustion. Applied Energy. 2017;208:1-11.
[54] Wissink ML, Splitter DA, Dempsey AB, Curran SJ, Kaul BC, Szybist JP. An assessment of thermodynamic merits for current and potential future engine operating strategies. Int J Engine Res. 2017;18:155-69.
[55] Matsuo S, Ikeda E, Ito Y, Nishiura H. The New Toyota Inline 4 Cylinder 1.8L ESTEC 2ZR-FXE Gasoline Engine for Hybrid Car. SAE Technical Paper 2016-01-0684; 2016.

Contact Information

szybistjp@ornl.gov

Acknowledgments

The authors gratefully acknowledge the support of the US Department of Energy Vehicle Technologies Office, particularly program managers Gurpreet Singh and Mike Weismiller.

The authors also gratefully acknowledge Brian Kaul at ORNL for his support with the unique control and data acquisition requirements for the experimental configurations used in this investigation.

Definitions/Abbreviations

AKI	Anti-knock index
aTDC$_f$	After firing top dead center
BMEP	Brake mean effective pressure
bTDC$_f$	Before firing top dead center
BTE	Brake thermal efficiency
CA	Crank angle
CA05	5% mass fraction burned
CA50	50% mass fraction burned
CA95	95% mass fraction burned
D-EGR	Dedicated EGR
EGR	Exhaust gas recirculation
ESU	Exhaust stroke utilization
LPG	Liquified petroleum gas
MON	Motor octane number
ORNL	Oak Ridge National Laboratory
PCI	Precision Combustion, Inc.
PFI	Port fuel injection
$\dot{Q}_{HR}$	Rate of heat release
POx	Partial oxidation
r_c	Compression ratio
RON	Research octane number
SI	Spark ignition
TCR	Thermochemical recuperation
WGS	Water-gas shift
Φ	Equivalence ratio